

1 **Identification of dominant ADCC epitopes on hemagglutinin antigen of pandemic H1N1**
2 **influenza virus**

3
4 **Vikram Srivastava^{a#}, Zheng Yang^{a#}, Ivan Fan Ngai Hung^b, Jianqing Xu^c, Bojian**
5 **Zheng^a, Mei-Yun Zhang^{a,1}**

6
7 ^aDepartment of Microbiology, ^bDepartment of Medicine, Li Ka Shing Faculty of Medicine,
8 The University of Hong Kong, Hong Kong, China

9 ^cInstitutes of Biomedical Sciences, Shanghai Public Health Clinical Center, Fudan
10 University, Shanghai 201508, China

11
12
13
14 Running title: Dominant ADCC epitopes on influenza virus HA

15
16 ¹**To whom correspondence should be addressed:**

17 **Mei-Yun Zhang, PhD**

18 AIDS Institute, Department of Microbiology

19 Li Ka Shing Faculty of Medicine, The University of Hong Kong

20 L5-45, Laboratory Block, 21 Sassoon Road, Pokfulam

21 Hong Kong, China.

22 Phone: 852-28183685; Fax: 852-28177805; Email: zhangmy@hku.hk

23
24 # contributed equally to this work

25
26

27 **ABSTRACT**

28 Antibody-dependent cell-mediated cytotoxicity (ADCC) bridges innate and adaptive
29 immunity, and it involves both humoral and cellular immune responses. ADCC has been
30 found to be a main route of immune protection against viral infections in vivo.
31 Haemagglutinin (HA) of influenza virus is highly immunogenic and considered the most
32 important target for immune protection. Several potent cross-reactive HA-specific
33 neutralizing monoclonal antibodies (mAbs) have been reported and their conserved
34 neutralizing epitopes revealed, but there has been no report so far about ADCC epitopes on
35 HA. Here we identified two dominant ADCC epitopes, designated E1 [Amino acid (AA) 92-
36 117] and E2 (AA 124-159), on HA of pandemic H1N1 influenza virus by epitope mapping of
37 convalescent plasma IgGs from six H1N1-infected human subjects in China that exhibited
38 different levels of ADCC activity. E1 and E2 ADCC epitopes overlapped with
39 immunodominant epitopes of HA. Depletion of purified patient plasma IgGs with yeast cells
40 expressing E1 or E2 peptides decreased ADCC activity of the IgGs. E1 and E2 sequences
41 were found to be highly conserved in H1N1 strains, but less so in other subtypes of influenza
42 A viruses. Our study may aid in designing immunogens that can elicit antibodies with high
43 ADCC activity. Vaccine immunogens designed to include the structural determinants of
44 potent broadly neutralizing Abs and ADCC epitopes may confer a comprehensive immune
45 protection against influenza virus infection.

46

47 INTRODUCTION

48 Influenza virus infection is one of the most common causes of serious respiratory illness. The
49 outbreak of a novel H1N1 influenza virus in the year 2009 revitalized the interest to
50 understand epidemiological and immunological aspects of influenza virus. Virus infection
51 induces various immune responses, of which humoral immune responses are primarily
52 responsible for preventive and protective immunity (1, 2). Antibodies against viral antigens
53 may provide protection either by Fab-mediated neutralizing effect which may interfere with
54 the binding of virus to the cell surface receptor(s) or block other functionally important viral
55 structures, or by Fc-mediated effector functions, including antibody-dependent cell-mediated
56 cytotoxicity (ADCC), phagocytosis, and complement-dependent cytotoxicity (CDC), which
57 destroy the infected cells. It has been reported that broadly HIV-1-neutralizing human mAb
58 b12 decreased viral load through ADCC, but not CDC, in passive immunization of rhesus
59 macaques (3). A follow-up study of the recent RV144 phase III HIV-1 vaccine trial that
60 demonstrated 31.2% efficacy also suggested that the high level ADCC activity of plasma
61 samples of the vaccinees inversely correlated with infection risk (4, 5). ADCC against
62 influenza virus-infected cells was first described by Greenberg et al (6). It was well
63 documented that the ADCC-mediated clearance of virus-infected cells occurred before
64 infectious virus particles were released from the infected cells and before other immune
65 responses, humoral or cellular, were initiated (7). Considering the fact that the ADCC
66 invokes protective immune response against viral infection (8), ADCC antibody response was
67 incorporated as one of the important characteristics of potential vaccine candidate by World
68 Health Organization (9).

69 A number of HA-specific potent broadly neutralizing mAbs (bnmAbs) have been
70 reported (10-16). They target conserved epitopes either on HA2 that mediates viral fusion or
71 on the globular head region HA1 that interacts with the receptor. For example, HA2-specific
72 bnmAbs CR6261 and F10 recognize conformational epitopes within the conserved A helix,

73 while HA2-specific bnmAb 12D1 recognizes a linear epitope within the long CD helix (10,
74 12, 15). HA1-specific bnmAb 5J8 neutralizes a broad spectrum of 20th century H1N1 viruses
75 and influenza A(H1N1)pdm virus, and it recognizes a novel and conserved epitope between
76 the receptor-binding pocket and the Ca2 antigenic site (13). Another HA1-specific mAb C05
77 neutralizes strains from multiple subtypes of influenza A virus, and it recognizes conserved
78 elements of the receptor-binding site by a single long heavy-chain complementarity-
79 determining region 3 (HCDR3) loop (14). Like HIV-1 specific bnAbs, influenza virus HA-
80 specific bnAbs are infrequently elicited in natural infection or by vaccine immunization.
81 Among all influenza virus HA-specific bnmAbs, CH65 may be the only mAb that was
82 isolated from a vaccinee. CH65 also recognizes the receptor binding pocket on HA1,
83 mimicking in many aspects the interaction of the physiological receptor, sialic acid, with
84 HA1 (16). Whether these HA-specific bnmAbs provide immune protection through ADCC
85 remains to be determined. There has been no report so far about ADCC epitope(s) of
86 influenza virus HA antigen and their immunogenicity. In this study we screened a panel of
87 convalescent plasma samples obtained from H1N1-infected human subjects, and identified
88 two samples with high ADCC activity against pandemic H1N1 influenza virus by using a
89 fluorescence-based ADCC assay. We did epitope mapping of these two samples, as well as
90 three other plasma samples with moderate to weak ADCC activity and one plasma sample
91 with no ADCC activity by using purified IgGs and yeast display technology. We delineated
92 potential dominant ADCC epitopes by comparing the mapping patterns against different IgG
93 samples with different levels of ADCC activity.

94

95 **MATERIALS AND METHODS**

96 **Cell lines, media and reagents.** The Raji (CCL-86) cell line was obtained from American
97 Type Culture Collection (ATCC) and maintained in RPMI 1640 (Invitrogen) containing 10%
98 heat-inactivated fetal calf serum (FCS) and 2% L-glutamine at 37°C with 5% CO₂. The

99 following reagents were purchased: penicillin/streptomycin (Sigma), PE labelled anti-human
100 IgG (Fab')₂ (Jackson ImmunoResearch), FITC labelled anti-c-myc mouse IgG (Sigma), and
101 fluorescent dyes PKH-67 (Sigma) and 7-AAD (Invitrogen).

102 **Convalescent plasma samples from H1N1-infected human subjects.** This research
103 was authorized by the Institutional Review Board of the University of Hong Kong / Hospital
104 Authority Hong Kong West Cluster (IRB reference number: UW 11-351). All archived
105 plasma samples used in the study were obtained from the patients infected with influenza
106 A(H1N1)pdm virus, which were confirmed by either RT-PCR or viral culture (17). The
107 median time of plasma collection from the date of onset of infection was 16 months.

108 **Purification of plasma IgGs.** Polyclonal IgGs were purified from plasma samples by
109 Protein G affinity purification. Briefly, plasma samples were thawed, heat inactivated at 56°C
110 for 45 min, clarified by centrifugation, and filtered through a 0.2 µm mini capsule filter before
111 loaded onto a Protein G Sepharose column (GE Biosciences) equilibrated with PBS. IgGs
112 were eluted with 0.5 M acetic acid (pH 3.0), immediately neutralized with 3M Tris (pH 9.0),
113 and dialysed against PBS. The purity of polyclonal IgGs was confirmed by reducing and non-
114 reducing SDS-PAGE.

115 **Hemagglutination-inhibition (HAI) assay.** HAI assay was performed in V-bottom
116 96-well microtiter plates as previously described (18). Briefly, non-specific inhibitors were
117 inactivated by treating each aliquot of plasma sample with receptor destroying enzyme (RDE)
118 (Denka Seiken, Japan) at a ratio of 1:3 (RDE/plasma) at 37°C overnight. The enzyme was
119 heat inactivated by incubation at 56°C for 30 min. Samples were 2-fold serially diluted with
120 a starting dilution of 1:10. An equal volume of the pandemic H1N1 A/HK/01/2009 virus,
121 adjusted to approximately 4 HA units/50 µl was added to each well. The plates were covered
122 and incubated at RT for 1 h followed by addition of 0.5% turkey erythrocytes to the plasma
123 /virus mixture and further incubation at room temperature for 30 min.

124 **Neutralization assay.** The micro-neutralization assay for the pandemic H1N1
125 A/HK/01/2009 was carried out in microtiter plates with neutralization of the virus cytopathic
126 effect as the endpoint in Madin-Darby canine kidney (MDCK) cells described previously
127 (18). Briefly, serially diluted plasma samples in duplicate with a starting dilution of 1:10 were
128 mixed with the virus with 100 50% tissue culture infective doses. Following incubation at
129 37°C for 2h, the plasma / virus mixture were added to MDCK cells. 1 h post infection, the
130 mixtures were removed, and plasma-free minimal essential medium containing 2 µg/ml of
131 TPCK (L-1-tosylamide-2-phenylethyl chloromethyl ketone)-treated trypsin (TPCK-Trypsin;
132 Sigma Immunochemical) was added to each well. The plates were incubated at 37°C for 3-4
133 days, and the cytopathic effect was recorded and the highest plasma dilution that protected
134 ≥50% of the cells from cytopathology in the wells determined. Positive and negative controls
135 and virus back titration for confirmation of the viral inoculum were included in each assay.

136 **Preparation of infected target cells.** Raji cells were used as target cells in the ADCC
137 assay and infected target cells prepared as follow. Briefly, Raji lymphoblasts (19) cells were
138 infected with influenza virus H1N1 A/California/04/2009 at a multiplicity to give about 80-
139 95% infected cells. A sample of target cells was removed 48 h post infection in order to
140 assess the percent infected cells based on the ability of infected cells to produce
141 hemadsorption with turkey red blood cells (RBCs), or by flow cytometry using purified IgGs
142 from H1N1-infected patients.

143 **Flow cytometry of infected target cells.** Infected cells were washed twice with PBS
144 by centrifugation at 400 x g for 5 min, incubated with 5 µg/ml purified IgGs at 4°C for 2 h
145 followed by washing thrice with FACS buffer (1% BSA in PBS). The cells were then
146 incubated with PE conjugated to anti-human IgG, F(ab')₂ at 4°C for 1 h followed by washing
147 twice with FACS buffer and fixation with 2% paraformaldehyde in FACS buffer. The stained
148 cells were analyzed on a BD flow cytometer and results analyzed by FlowJo software.

149 **Preparation of effector cells.** Peripheral blood mononuclear cells (PBMCs) were
150 prepared by Ficoll-paque separation of heparinized whole blood obtained from healthy
151 volunteers and used as effector cells in the ADCC assay. Briefly, the heparinized whole blood
152 was diluted with an equal volume of PBS containing 10% FCS and 0.5%
153 penicillin/streptomycin (Pen/Strep). Blood was layered over Ficoll-Paque plus (GE
154 Healthcare) and centrifuged at 650 x g for 30 min. The PBMCs were harvested and washed
155 twice with PBS.

156 **ADCC assay.** ADCC activity was determined by a flow cytometry-based assay using
157 two fluorescent dyes to discriminate live and dead cells (20). PKH-67, a membrane labelling
158 dye, was used to specifically identify the target cells. PKH-67 binds to the cell membrane,
159 and the dye remains on the cell membrane, even after cell death, avoiding cross-
160 contamination with effector cells. 7-amino-actinomycin-D (7-AAD) is excluded by viable
161 cells, but can penetrate the cell membrane of dead or dying cells, and intercalate into double
162 stranded DNA. Briefly, PKH-67-labelled target cells and unlabelled effector cells were
163 prepared in RPMI 1640 medium containing 10% FCS and 0.5% Pen/Strep to a cell density of
164 1×10^6 cells/ml and 2.5×10^7 cells/ml, respectively. Purified IgGs were diluted to 5 μ g/ml and
165 1 μ g/ml in PBS. 50 μ l of target cells were dispensed into a round-bottom 96-well plate in
166 duplicate followed by addition of 50 μ l of 5 μ g/ml or 1 μ g/ml IgGs, resulting in a final
167 concentration of 2.5 μ g/ml or 0.5 μ g/ml IgGs. In the case of plasma samples used in the
168 assay, plasma samples were diluted to a final dilution of 1:2,000 or 1:10,000. Following
169 incubation at 37°C for 15 min, 100 μ l of effector cells were added to the target cells / IgG or
170 plasma mixture. Effector cells (pooled PBMCs from three healthy volunteers) and target cell
171 solutions containing no IgG and IgGs from healthy volunteers were also prepared as controls.
172 Following 2 h incubation, 1 μ l of 7-AAD was added to the wells. Cell death was determined
173 on a FACS AriaIII flow cytometer using BD FACS Diva software (BD Biosciences, USA). A
174 total of 5,000 target cells were acquired. Percent cell death was determined by software

175 analysis of four identifiable cell populations, live effector cells (no dye), dead effector cells
176 (7-AAD positive), live target cells (PKH-67 positive) and dead target cells (PKH-67 and 7-
177 AAD double positive). Assay controls used to define cell populations included target cells
178 alone (background cell death) and target cells with 5 μ l Triton X-100 added (maximum
179 fluorescence). Percent ADCC was calculated as $[(\% \text{ experimental lysis} - \% \text{ spontaneous}$
180 $\text{ lysis}) / (\% \text{ maximum lysis} - \% \text{ spontaneous lysis})] \times 100$, in which “% spontaneous lysis”
181 referred to percent lysis of infected cells with effectors in the absence of plasma or IgGs, and
182 “% maximum lysis” referred to percent lysis of infected cells with effectors in the presence of
183 1% Triton X-100. Experiments were performed in duplicate and repeated once. One
184 representative set of data was shown in this report.

185 **Construction of HA fragments yeast-displayed library.** The gene encoding the
186 full-length HA of influenza virus H1N1 A/HK/01/2009 was amplified by PCR using a
187 recombinant plasmid containing the full length HA gene as template and a pair of primers,
188 HAF (5'-atgaaggcaataactagtagttc-3') and HAR (5'-ttaaatacatattctacactg-3') (21). 2 μ g of gel-
189 purified HA PCR products was digested with 0.9 units of DNase I (Roche) at 15°C for 15
190 min in a total volume of 50 μ l digestion buffer (50 mM Tris-HCl, pH 7.5, 10 mM MnCl₂).
191 The reaction was stopped by adding EDTA to a final concentration of 50 mM followed by
192 flash freezing in liquid nitrogen and incubation at 90°C for 10 min to inactivate DNase I.
193 Randomly digested PCR products were analysed on 2% agarose gel and fragments ranging
194 from 100 bp to 500 bp in size gel extracted. The gel-purified fragments were blunt ended by
195 using T4 DNA polymerase (New England Biolabs), and ligated to a modified pComb3X
196 vector (the multiple cloning sites between two Sfi I sites were replaced with a SmaI
197 restriction site) digested with Sma I. The blunt end ligation products were electroporated into
198 TG1 electrocompetent cells, resulting in an HA fragment bacteria library. Recombinant
199 plasmids were large-scale prepared from the bacteria library using plasmid Maxi-prep kit
200 (QIAGEN) and the inserts amplified by PCR using three sense primers, 3XYDF1 (5'-

201 tattttctgttattgcttcagttttggcccaggcggcc-3'), 3XYDF2 (5'-
202 tattttctgttattgcttcagttttCggcccaggcggcc-3') and 3XYDF3 (5'-
203 tattttctgttattgcttcagttttCCggcccaggcggcc-3'), paired with three antisense primers, 3XYDR1
204 (5'-accctcagagccaccactagttggccggcctggcc-3'), 3XYDR2 (5'-
205 accctcagagccaccactagttggccggcctggcc-3') and 3XYDR3 (5'-
206 accctcagagccaccactagttGggccggcctggcc-3'). Each sense primer was paired with each
207 antisense primer in the PCRs in order to avoid any clonal loss resulting from open-reading
208 frame shift either in the fragment region or in the C-terminal myc tag region or both in the
209 final yeast display library. All PCR products were gel-purified and re-amplified by PCR
210 using high-fidelity DNA polymerase (Invitrogen) and a pair of primers, YDRDF (5'-
211 ctctcgtgttttcaatattttctgttattgcttcag-3') and YDRDR (5'-
212 gagccgccaccctcagaaccgccaccctcagagccaccactag-3'), to add two overhang regions for
213 homolog recombination with linearized yeast display plasmid pYD7, a modified vector of
214 pCTCON2 (22). The following PCR program was used for re-amplification of the inserts: an
215 initial denaturation at 95°C for 3 min followed by 20 cycles of (95°C, 30s, 58°C, 30s, 72°C,
216 30s) and a final extension at 72°C for 10 min. The amplified inserts were mixed with
217 linearized PYD7 plasmid DNA at a ratio of 3:1 (12 µg of inserts were mixed with 4 µg of
218 linearized pYD7), and electroporated into yeast competent cells, EBY100, by the Li-Ac
219 method (23). The resultant yeast library contained 5 million individual recombinant yeast
220 clones. Following amplification, recombinant yeast cells were aliquoted and preserved in
221 SDCAA medium supplemented with 15% glycerol at -80°C. Each aliquot contained 100
222 million yeast cells in 1 ml frozen medium.

223 **Yeast library sorting and flow cytometry of monoclonal yeast.** Induction of
224 expression of HA fragments on yeast cell surface was performed by following the protocol
225 provided by Wittrup's group (22). Recombinant yeast cells were grown in SDCAA medium
226 (yeast nitrogen-based casamino acid medium containing 20 g/l glucose) at 30°C for 24 h with

227 shaking and passaged once with fresh medium to eliminate dead cells. The yeast cells were
228 centrifuged and resuspended in SGCAA medium (yeast nitrogen-based casamino acid
229 medium containing 20g/l galactose) to an optical density at 600 nm (OD_{600nm}) of 0.5-1.0,
230 and then induced at 20°C for 36-48 h with shaking. The induced yeast population were
231 subject to sorting against purified IgGs as follow. The induced recombinant yeast population
232 were stained with a final concentration of 500 nM purified IgGs by incubation at 4°C for 3 h.
233 Following washing twice with cold PBS, yeast cells were incubated with PE conjugated to
234 goat anti-human IgG, (Fab')₂ and FITC conjugated to mouse anti-c-myc IgG at 4°C for 1 h.
235 Following washing thrice with cold PBS, yeast cells were sorted using FACS Aria III (BD
236 Biosciences) for PE and FITC double positive populations. PE and FITC labelled beads and
237 unstained yeast library were used for calculation of compensation prior to sorting. The same
238 gate was used for sorting recombinant yeast library stained with different polyclonal IgGs.
239 For each polyclonal IgG sample 3-5×10⁵ yeast cells were sorted. Double positive population
240 were verified by flow cytometry of randomly picked monoclonal yeast from the population
241 using the same primary and secondary antibodies as described above.

242 **DNA sequencing and epitope mapping.** Recombinant yeast plasmids were extracted
243 from each sorted yeast library using yeast cell plasmid extraction kit (Omega Bio-Tek) and
244 electroporated into *E. coli* TG1 electrocompetent cells. More than 300 ampicillin resistant
245 yeast clones from each sorted library were sequenced using primers annealing to pYD7 and
246 the sequences analysed. The recombinant clones with the inserts in the HA open-reading
247 frame and with productive Aga2-C-myc tag were considered positive clones. The deduced
248 amino acid (AA) sequences of positive clones were used for epitope mapping
249 (<http://insilico.ehu.es/translate/>) against HA sequence of Influenza virus H1N1
250 A/HK/01/2009 (GenBank: ACR18920.1). The insert sequences with less than 4 AAs in
251 length, or identity rate below 75%, were excluded from the analysis. About 100-150 valid
252 positive clones were identified for each plasma IgG sample. The frequency of each AA

253 presented in the valid positive clones was counted and calibrated for the same total number of
254 5,000 AAs for each IgG sample.

255 **Depletion of purified IgGs with recombinant yeast expressing E1 or E2.** 10^8
256 recombinant yeast cells surface-displaying E1 or E2 were washed with PBS twice by
257 centrifugation at 2000 x g for 5 min, and incubated with 500 μ g of IgGs M1036 or M1037 at
258 a total volume of 1 ml in PBS at 4°C overnight. Yeast cells were pelleted by centrifugation at
259 2000 x g for 5 min and the supernatant transferred to a new preparation of 10^8 recombinant
260 yeast cells surface-displaying E1 or E2 and incubated at RT for 1 h. Yeast cells were pelleted
261 by centrifugation at 2000 x g for 5 min and the supernatant collected in new tubes. Sequential
262 depletion with E1 and E2 was carried out by switching the recombinant yeast expressing E1
263 or E2 in the second round of depletion followed by additional round of depletion with the
264 same recombinant yeast. Antibody concentrations in the depleted IgG samples were
265 determined by measuring OD280nm using Nanodrop.

266

267 **RESULTS**

268 **Characterization of patient plasmas.** Seven convalescent plasma samples were
269 characterized for hemagglutination inhibition (HAI) and neutralization activities (Fig. 1). All
270 plasma samples had an HAI titre \geq 1:160, with plasma M1024 having the highest HAI titre of
271 1:1,280 (Fig. 1). All plasma samples showed similar neutralization endpoint dilution (NI)
272 titers. Plasma M1017 and M1039 had an NI titer of 1:160, while all others 1:320 (Fig. 1).
273 Polyclonal antibodies were purified from these plasma samples and the binding of purified
274 IgGs to H1N1-infected target cells confirmed by flow cytometry (Fig. 2). All IgG samples
275 showed similar binding activity at 10 μ g/ml except that M1081 IgGs showed relatively high
276 binding to the infected target cells (Fig. 2). ADCC activity of 1:10,000 and 1:2,000 diluted
277 plasmas was then measured by a flow cytometry-based ADCC assay. Percent increase in
278 cytotoxicity of infected target cells in the presence of five out of seven diluted plasma

279 samples was observed (Fig. 3A). Three plasma samples, M1036, M1037 and M1024,
280 exhibited high cytotoxicity activity at one or both dilutions. Plasma M1039 and M1081 also
281 showed cytotoxicity activity that was above the average (%ADCC=10%), while the
282 remaining two plasma samples, M1017 and M1089, did not show ADCC activity. To confirm
283 that the IgGs in the plasma samples contributed to the observed cytotoxicity, purified IgGs at
284 concentrations (0.5 µg/ml and 2.5 µg/ml) that were equivalent to the antibody concentrations
285 in the diluted plasmas were tested in the same ADCC assay (Fig. 3B). The result was largely
286 consistent with that using the diluted plasma. Five out of seven samples, IgGs M1036,
287 M1037, M1039, M1017 and M1024, had above-average ADCC activity (10%) at one or both
288 antibody concentrations, while two samples, IgGs M1081 and M1089 had below average
289 cytotoxicity (Fig. 3B). Discrepancy between the two sets of data was observed with sample
290 M1017. Plasma M1017 had no or negative cytotoxicity, but its purified IgGs had above
291 average cytotoxicity (Fig. 3). Based on the percent ADCC tested with the purified IgGs, we
292 categorized six IgG samples into three groups: ADCC++ (M1036, M1037), ADCC+ (M1017,
293 M1024 and M1039), and ADCC- (M1089). All six IgG samples were subject to epitope
294 mapping by yeast display. Sample M1081 was excluded in the further analysis for its below
295 average or negative ADCC activity in both assays.

296 **Construction of recombinant yeast library and sorting induced yeast library**
297 **against six IgG samples.** To assess the quality of HA fragments recombinant yeast library,
298 we sent over 100 random yeast clones for DNA sequencing. The inserts with a length ranging
299 from 50 bp to 750 bp and an average length of 146 bp were distributed over the full length
300 HA ectodomain with no significant bias to certain region(s) although two hot spots at AA
301 position 162-179 and 464-481 were observed (data not shown). The yeast library was induced
302 to express HA fragments on cell surface and the induced yeast library stained were incubated
303 with individual IgG samples as a primary antibody and PE-anti-human IgG, F(ab')₂ and
304 FITC-anti-c-myc as secondary antibodies. PE and FITC double positive yeast cells were

305 sorted and amplified. 20-30 monoclonal yeast were randomly picked from each sorted library
306 and tested by flow cytometry for expression of c-myc and for binding to the IgG sample used
307 for sorting. About 50 % monoclonal yeast clones were positive for binding to the IgGs (mean
308 value two times higher than mouse IgG isotype control). All positive yeast clones were sent
309 for DNA sequencing, and 35-50 % of which had an insert that was in HA open reading frame.
310 Based on the small scale sequencing result, a total of 300-350 monoclonal yeast were picked
311 from each sorted library and sent for DNA sequencing, and about 100-150 valid positive
312 clones were obtained from each sorted library.

313 **Epitope mapping of purified IgGs and identification of dominant ADCC epitopes**
314 **on H1N1 HA.** For each IgG sample, the AA sequences of all valid positive clones were
315 mapped to the HA sequence of Influenza virus H1N1 A/HK/01/2009 (GenBank:
316 ACR18920.1) and the frequency of each AA counted and calibrated, so that for each IgG
317 sample there were 5,000 AAs in total. The calibrated AA frequencies for each IgG sample
318 were then plotted onto H1N1 HA sequence (Fig. 4A). We observed three immunodominant
319 epitopes that had an average AA frequency over 10 for three or more IgG samples. Two
320 immunodominant epitopes, HA-E1 (AA 92-117) and HA-E2 (AA 124-159), were located on
321 HA1 region, and the third one, HA-E3 (AA 470-521), on HA2 region. To localize ADCC
322 epitopes, the calibrated AA frequencies for each position within the same ADCC group were
323 averaged and the averaged AA frequencies for each ADCC group re-plotted (Fig. 5B). The
324 first two immunodominant epitopes, HA-E1 and HA-E2, had an average AA frequency that
325 was two-fold higher in the ADCC++ or ADCC+ group than that in the ADCC- group
326 (TABLE 1), suggesting that HA-E1 and HA-E2 may be two dominant ADCC epitopes. The
327 third immunodominant epitope HA-E3 showed an average AA frequency that was more than
328 two-fold higher in the ADCC- group than that in the ADCC++ or ADCC+ groups (TABLE 1).

329 **Confirmation of dominant ADCC epitopes on HA.** To confirm possible ADCC
330 epitopes, we expressed HA-E1 and HA-E2 on yeast cell surface and used the recombinant

331 yeast to absorb two IgG samples in ADCC++ group, IgGs M1036 and M1037. The IgGs
332 absorbed with HA-E1 or HA-E2 alone showed significantly decreased ADCC activity
333 compared to the original IgG samples and the IgGs absorbed with HA-E3 expressed on yeast
334 cell surface (Fig. 5). Sequential absorption with recombinant yeast expressing HA-E1 and
335 HA-E2 almost abolished the ADCC activity of the two IgG samples, confirming that HA-E1
336 and HA-E2 may be dominant ADCC epitopes on HA and antibodies specific for HA-E1 and
337 HA-E2 peptides may have high ADCC activity (Fig. 5). We observed that IgG 1037 absorbed
338 with E3-expressing yeast also showed decrease in ADCC activity, presumably due to the
339 removal of E3-binding antibodies that may affect the ADCC activity, but the decrease in
340 ADCC activity caused by the absorption with E1 or E2-expressing yeast was more than 2-
341 fold more.

342 **Conservation of HA-E1 and HA-E2 epitopes.** We first analyzed the conservation
343 rate of HA-E1 and HA-E2 sequences in H1N1 strains circulating in 2007-2009. A total of
344 2408 H1N1 HA sequences downloaded from Los Alamos Influenza Research Database
345 (<http://www.fludb.org/brc/home.do?decorator=influenza>) were included in the analysis
346 (TABLE 2). We found that both E1 and E2 were highly conserved in 2009_H1N1 strains
347 with average AA conservation rate reached 95% and 94%, respectively. E1 and E2 were
348 relatively conserved in 2007_ and 2008_H1N1 strains with average AA conservation rate
349 over 70%. Mutations occurred mainly at 6 AA positions of E1 and 11 of E2 with a
350 conservation rate of each AA below 15% (TABLE 2). We then analyzed the conservation
351 rate of E1 and E2 in 2,325, 1,339 and 7,880 influenza A viruses (IFA) isolated in 2007, 2008
352 and 2009, respectively. A total of 11,544 IFA HA sequences downloaded from the Los
353 Alamos Influenza Research Database were included in the analysis (TABLE 2). We found
354 that both E1 and E2 were also conserved in IFAs circulating in 2009 with an average
355 conservation rate over 80%, but much less so in IFAs circulating in 2007 and 2008 with an
356 average conservation rate below 60% (TABLE 2). We found that a few residues in E1 and E2

357 were well conserved with no change in all reported HA sequences of IFAs, including E98,
358 C107, Y108 and P109 in E1, and G148 and C153 in E2 (TABLE 2), suggesting their
359 importance for HA structural integrity and / or function.

360

361 **DISCUSSION**

362 Both neutralizing and non-neutralizing antibodies may confer cytotoxicity effect largely
363 depending on antibody affinity for Fc gamma receptors (FcRrs) (24-28). The four subclasses
364 of human IgG differ from each other in the cytotoxic potency due to their different affinities
365 for FcRrs. In general, the rank order is IgG1 (++++) = IgG3 (+++) > IgG2 (+/-) ≥ IgG4 (+/-)
366 for ADCC. IgG1 and IgG3-mediated ADCC rely on FcRRIIIa that mainly expresses on NK
367 cells and FcRI that expresses on monocytes. Although ADCC activity is mediated by the Fc
368 region, the Fab region of IgG that binds to the antigen expressed on the surface of target cells
369 may affect Fc-mediated ADCC activity (29, 30). The mechanism for Fab effect on ADCC
370 remains to be elucidated. In this study, we purified plasma antibodies by using Protein G
371 affinity column, which purified all four IgG subclasses. In human sera, IgG1 is the most
372 abundant subclass and accounts for 66% of total IgGs, while IgG2, IgG3, IgG4 account for
373 23%, 7% and 4%, respectively. Therefore, the ADCC activity detected in this study was
374 mediated mainly by IgG1s. Similar binding activity of purified IgGs to H1N1-infected Raji
375 cells as measured by flow cytometry suggests that different ADCC activities of different
376 convalescent plasma IgG samples may be attributed to different epitopes recognized by the
377 purified IgGs. Two dominant ADCC epitopes on HA were identified by differential epitope
378 mapping of plasma IgGs with different ADCC activities, and confirmed by using epitope-
379 expressing recombinant yeast depleted IgGs in the same ADCC assay. E1 has 26 AAs and E2
380 36 AAs in length, suggesting that they may not be a single epitope, but multiple epitopes
381 instead, and that both E1 and E2 may not be linear epitopes. Depletion of plasma IgGs with
382 E2-expressing recombinant yeast seems more effective than that with E1-expressing

383 recombinant yeast (Fig. 5), suggesting that E2 may be more important than E1 in eliciting
384 antibodies with ADCC activity. The seven human individuals were infected with same H1N1
385 strain, but the ADCC activity of their plasmas and purified IgGs were different, and the
386 difference did not seem to correlate with the HAI and NI titers of the plasma (Fig. 1 and 3).
387 The mechanism for the different antibody profiles and different ADCC activities in different
388 individuals infected with the same virus strain requires further study. The patients included in
389 this study presented mild symptoms and recovered from influenza virus infection during the
390 outbreak of swine flu in 2009. Their plasma had a similar NI titre, but different ADCC
391 activity. It would be interesting to determine how much the ADCC activity of the plasma
392 IgGs contribute to the control of virus infection. We observed that patient M1024 plasma had
393 an HAI titer which was significantly higher than that of other plasmas, but purified IgG
394 M1024 showed moderate ADCC activity and an average neutralization activity. It would be
395 also interesting to determine if and how HAI activity of the plasma contributes to the control
396 of virus infection. The discordance between HAI and neutralization assay results has been
397 observed in our previous study (18), and could be explained by several mechanisms. The HAI
398 assay measures HA-specific antibodies in binding to HA and interfering with virus
399 agglutination with RBC, while the neutralization assay using live virus measures the capacity
400 of total antibodies (not only HA-specific antibodies) for inhibiting the entry of virus to target
401 cells. The antibodies that neutralize virus may not inhibit hemagglutination and hence are not
402 detected by the HAI assay. Similarly, antibodies that inhibit hemagglutination may not have
403 viral neutralizing activity and therefore are not detectable by the neutralization assay. In
404 addition, virus strains, host source of the red blood cells and other non-specific inhibitors may
405 also affect the binding avidity in HAI assay. Sequence conservation analysis showed that E1
406 and E2 were highly conserved in H1N1 strains. Although the conservation rates of E1 and E2
407 were not high in other subtypes of influenza A viruses, we identified some well conserved
408 residues in both E1 and E2, which may be useful for designing subtype-specific vaccine

409 immunogens. The identification of dominant ADCC epitopes on H1N1 HA shown in this
410 study may help develop universal vaccine that confers comprehensive protection against
411 influenza virus infection.

412 In this study, we used H1N1-infected target cells in the ADCC assay. Both HA and
413 neuraminidase (NA) were antigenic determinants for ADCC antibodies, but NA was found to
414 be a minor ADCC determinant (31). The ectodomain of matrix protein 2 (M2e) of influenza
415 A virus has been suggested to be an attractive target for a universal influenza A vaccine
416 because M2e sequence is highly conserved in influenza virus subtypes. Intraperitoneal or
417 intranasal administration of M2e-based proteins / particles to mice provided 90-100%
418 protection against a lethal virus challenge and the protection was mediated by antibodies (32,
419 33). But the immunogenicity of M2e alone is very weak and natural infection with influenza
420 A viruses usually does not induce significant M2e-specific antibodies. We tested the binding
421 of all seven convalescent plasma IgGs to recombinant M2e by ELISA and the titers were
422 overall low (data not shown). We cannot exclude the possibility that M2e-specific antibodies
423 present in IgGs M1036 and M1037 may contribute to the killing of H1N1-infected cells, but
424 considering the overall low titer of M2e-specific antibodies in the plasmas, and supposedly
425 restricted accessibility of M2e-specific antibodies to M2 on the infected cell surface in the
426 presence of HA-specific antibodies, we assume that M2e-specific antibody mediated ADCC
427 activity in IgGs M1036, M1037 and other IgG samples may be minimal.

428 Various ADCC assays have been reported that differ mainly in the usage of effector
429 cells and measurement of ADCC activity. The most popular assay was the radioactive
430 chromium (^{51}Cr)-release assay, which was first developed in 1968 (34). The assay was based
431 upon the passive internalization and binding of ^{51}Cr of sodium chromate to target cells. Lysis
432 of the target cells by effector cells resulted in the release of the radioactive probe into the cell
433 culture, which can be detected by a γ -counter. This assay was considered a 'gold standard' to
434 measure cell-mediated cytotoxicity. The ^{51}Cr release assay usually takes about 6 to 24h to

435 complete depending on the type of cells, amount of labelling and activity measurement. This
436 assay has a number of disadvantages, including low sensitivity, poor labelling and high
437 spontaneous release of isotope from some target cells. Additional problems with the ⁵¹Cr-
438 release assay include biohazard and disposal problems with the isotope. To avoid these
439 limitations several other methods have been developed to assess ADCC activity. These
440 assays are based on the release of nonradioactive compounds from target cells, or detection of
441 enzymatic activity in target cells, or cell-based assays to detect dying or dead target cells by
442 fluorometry or flow cytometry. In this study we tested convalescent human plasma and
443 purified polyclonal IgGs in a flow cytometry-based ADCC assay by differential identification
444 of live and dead cells. We used PBMCs from healthy donors as effector cells and directly
445 measured the dead infected cells in the presence of plasmas or IgGs. The 7AAD dye used in
446 this assay to discriminate live and dead or dying cells can easily pass through a dead or dying
447 cell and intercalate with DNA. Whereas the assays based on the release of nonradioactive
448 compounds and enzymes from target cells to culture medium require complete lysis of the
449 target cells (20). We used NK-resistant Raji cells as target cells in this study. Unlike MDCK
450 cells, influenza virus infected Raji cells do not grow fast and have low background cell death
451 in the absence of antibodies, which makes Raji an ideal cell line for the ADCC assay. In
452 contrast, influenza virus infected MDCK cells grow fast and massive cell death occurs in the
453 absence of antibodies, which gives rise to high background cell death and makes it very
454 difficult to optimize the conditions for the ADCC assay. In the present study, for some
455 samples, we observed that more diluted plasma exhibited higher ADCC activity than less
456 diluted plasma, and IgGs at a low concentration led to higher ADCC activity than the IgGs at
457 a high concentration (Fig. 3A, 3B). The same phenomenon was also observed in other studies
458 (29, 30). It has been reported that the overall concentration of polyclonal IgGs affect
459 inversely the ADCC effect. However, it varies with immune status of the subjects and epitope
460 availability on the surface of the target cells. There is no conclusive study indicating the

461 correlation of concentration of IgG with ADCC activity. Saturation of antibodies,
462 interference of non-ADCC antibodies present in the polyclonal antibodies, and variation of
463 PBMCs may all contribute to this phenomenon (25, 35, 36).

464

465 **ACKNOWLEDGEMENTS**

466 We wish to thank Kwok-Yung Yuen, Kelvin KW To for providing the patient plasmas,
467 Hong-Lin Chen and Zhiwei Chen for influenza virus H1N1 strains and the recombinant
468 plasmid containing the full-length H1N1 HA gene, Dimiter S Dimitrov and Zhongyu Zhu for
469 pYD7 yeast plasmid, and Martial Jaume for Raji cell line. We thank Kwok-Yung Yuen,
470 Kelvin KW To, Linqi Zhang, Qi Zhao, Li Liu and Jia Guo for helpful discussions, and Yanyu
471 Zhang and Jingjing Li for technical assistance! This work was supported by China 12th 5-year
472 Mega project (# 2012ZX10001006) and Small Project Funding (# 201109176176 and #
473 201007176258) from the University of Hong Kong to M-Y. Z.

474

475 **FIGURE LEGEND**

476 **FIG 1 HAI and NI titers of convalescent plasma samples from seven H1N1-infected**
477 **human subjects.** Each plasma sample was tested for anti-HA antibodies by HAI assay. The
478 NI titer was determined against pandemic H1N1 A/HK/01/2009 virus.

479 **FIG 2 Binding of purified IgGs to H1N1-infected Raji cells by flow cytometry.** All IgG
480 samples were tested at 10 µg/ml. Nonspecific IgG sample was a secondary antibody only
481 control (without a primary antibody added).

482 **FIG 3 Percent ADCC of seven convalescent plasma samples and their purified IgGs.**
483 (A): Plasma samples were diluted 1:10,000 and 1: 2,000. (B): Purified IgGs were tested at 0.5
484 µg/ml and 2.5 µg/ml. Each sample was tested in duplicate and the average standard variation
485 was 5% as displayed in the error bars.

486 **FIG 4 Epitope mapping of six purified IgG samples.** A: The AA frequencies for all six
487 IgG samples were mapped onto HA ectodomain. B: Six IgG samples were grouped into
488 ADCC++ (M1036 and M1037), ADCC+ (M1024, M1027 and M1039) and ADCC- (M1089)
489 samples, and the AA frequencies averaged in each group and mapped to H1N1 HA
490 ectodomain. Y axis represents the frequency of each AA in positive clones. X axis represents
491 AA position on H1N1 HA.

492 **FIG 5 Percent ADCC of IgGs M1036 and M1037 after depletion with monoclonal yeast**
493 **expressing E1, or E2, or both.** Each depleted IgG sample was tested at a final concentration
494 of 2.5 µg/ml. Undepleted IgGs M1036 and M1037, and IgGs M1036 and 1037 depleted with
495 recombinant yeast expressing E3 were included as controls.

496

497 REFERENCES

- 498 1. **Vijaykrishna D, Smith GJ, Pybus OG, Zhu H, Bhatt S, Poon LL, Riley S, Bahl J,**
499 **Ma SK, Cheung CL, Perera RA, Chen H, Shortridge KF, Webby RJ, Webster**
500 **RG, Guan Y, Peiris JS.** 2011. Long-term evolution and transmission dynamics of
501 swine influenza A virus. *Nature* **473**:519-522.
- 502 2. **Jegerlehner A, Schmitz N, Storni T, Bachmann MF.** 2004. Influenza A vaccine
503 based on the extracellular domain of M2: weak protection mediated via antibody-
504 dependent NK cell activity. *J Immunol* **172**:5598-5605.
- 505 3. **Hessell AJ, Hangartner L, Hunter M, Havenith CE, Beurskens FJ, Bakker JM,**
506 **Lanigan CM, Landucci G, Forthal DN, Parren PW, Marx PA, Burton DR.** 2007.
507 Fc receptor but not complement binding is important in antibody protection against
508 HIV. *Nature* **449**:101-104.
- 509 4. **Rerks-Ngarm S, Paris RM, Chunsuttiwat S, Prensri N, Namwat C,**
510 **Bowonwatanuwong C, Li SS, Kaewkungkal J, Trichavaroj R, Churikanont N, de**
511 **Souza MS, Andrews C, Francis D, Adams E, Flores J, Gurunathan S, Tartaglia J,**
512 **O'Connell RJ, Eamsila C, Nitayaphan S, Ngaay V, Thongcharoen P, Kunasol P,**
513 **Michael NL, Robb ML, Gilbert PB, Kim JH.** 2012. Extended Evaluation of the
514 Virologic, Immunologic, and Clinical Course of Volunteers Who Acquired HIV-1
515 Infection in a Phase III Vaccine Trial of ALVAC-HIV and AIDSVAX B/E. *J Infect*
516 *Dis.*
- 517 5. **Rerks-Ngarm S, Pitisuttithum P, Nitayaphan S, Kaewkungwal J, Chiu J, Paris R,**
518 **Prensri N, Namwat C, de Souza M, Adams E, Benenson M, Gurunathan S,**
519 **Tartaglia J, McNeil JG, Francis DP, Stablein D, Birx DL, Chunsuttiwat S,**
520 **Khamboonruang C, Thongcharoen P, Robb ML, Michael NL, Kunasol P, Kim**
521 **JH.** 2009. Vaccination with ALVAC and AIDSVAX to prevent HIV-1 infection in
522 Thailand. *N Engl J Med* **361**:2209-2220.
- 523 6. **Greenberg SB, Criswell BS, Six HR, Couch RB.** 1977. Lymphocyte cytotoxicity to
524 influenza virus-infected cells. II. Requirement for antibody and non-T lymphocytes. *J*
525 *Immunol* **119**:2100-2106.

- 526 7. **Florese RH, Demberg T, Xiao P, Kuller L, Larsen K, Summers LE, Venzon D,**
527 **Cafaro A, Ensoli B, Robert-Guroff M.** 2009. Contribution of nonneutralizing
528 vaccine-elicited antibody activities to improved protective efficacy in rhesus
529 macaques immunized with Tat/Env compared with multigenic vaccines. *J Immunol*
530 **182:3718-3727.**
- 531 8. **Gomez-Roman VR, Patterson LJ, Venzon D, Liewehr D, Aldrich K, Florese R,**
532 **Robert-Guroff M.** 2005. Vaccine-elicited antibodies mediate antibody-dependent
533 cellular cytotoxicity correlated with significantly reduced acute viremia in rhesus
534 macaques challenged with SIVmac251. *J Immunol* **174:2185-2189.**
- 535 9. 1983. Immune responses to viral antigens in man and their relevance to vaccine
536 development: memorandum from a WHO meeting. *Bull World Health Organ* **61:935-**
537 **940.**
- 538 10. **Ekiert DC, Bhabha G, Elsliger MA, Friesen RH, Jongeneelen M, Throsby M,**
539 **Goudsmit J, Wilson IA.** 2009. Antibody recognition of a highly conserved influenza
540 virus epitope. *Science* **324:246-251.**
- 541 11. **Ekiert DC, Friesen RH, Bhabha G, Kwaks T, Jongeneelen M, Yu W, Ophorst C,**
542 **Cox F, Korse HJ, Brandenburg B, Vogels R, Brakenhoff JP, Kompier R, Koldijk**
543 **MH, Cornelissen LA, Poon LL, Peiris M, Koudstaal W, Wilson IA, Goudsmit J.**
544 2011. A highly conserved neutralizing epitope on group 2 influenza A viruses.
545 *Science* **333:843-850.**
- 546 12. **Sui J, Hwang WC, Perez S, Wei G, Aird D, Chen LM, Santelli E, Stec B, Cadwell**
547 **G, Ali M, Wan H, Murakami A, Yammanuru A, Han T, Cox NJ, Bankston LA,**
548 **Donis RO, Liddington RC, Marasco WA.** 2009. Structural and functional bases for
549 broad-spectrum neutralization of avian and human influenza A viruses. *Nat Struct*
550 *Mol Biol* **16:265-273.**
- 551 13. **Krause JC, Tsibane T, Tumpey TM, Huffman CJ, Basler CF, Crowe JE, Jr.**
552 2011. A broadly neutralizing human monoclonal antibody that recognizes a conserved,
553 novel epitope on the globular head of the influenza H1N1 virus hemagglutinin. *J Virol*
554 **85:10905-10908.**
- 555 14. **Ekiert DC, Kashyap AK, Steel J, Rubrum A, Bhabha G, Khayat R, Lee JH,**
556 **Dillon MA, O'Neil RE, Faynboym AM, Horowitz M, Horowitz L, Ward AB,**
557 **Palese P, Webby R, Lerner RA, Bhatt RR, Wilson IA.** 2012. Cross-neutralization
558 of influenza A viruses mediated by a single antibody loop. *Nature* **489:526-532.**
- 559 15. **Wang TT, Tan GS, Hai R, Pica N, Petersen E, Moran TM, Palese P.** 2010.
560 Broadly protective monoclonal antibodies against H3 influenza viruses following
561 sequential immunization with different hemagglutinins. *PLoS Pathog* **6:e1000796.**
- 562 16. **Whittle JR, Zhang R, Khurana S, King LR, Manischewitz J, Golding H,**
563 **Dormitzer PR, Haynes BF, Walter EB, Moody MA, Kepler TB, Liao HX,**
564 **Harrison SC.** 2011. Broadly neutralizing human antibody that recognizes the
565 receptor-binding pocket of influenza virus hemagglutinin. *Proc Natl Acad Sci U S A*
566 **108:14216-14221.**
- 567 17. **Hung IF, To KK, Lee CK, Lee KL, Chan K, Yan WW, Liu R, Watt CL, Chan**
568 **WM, Lai KY, Koo CK, Buckley T, Chow FL, Wong KK, Chan HS, Ching CK,**
569 **Tang BS, Lau CC, Li IW, Liu SH, Chan KH, Lin CK, Yuen KY.** 2011.
570 Convalescent plasma treatment reduced mortality in patients with severe pandemic
571 influenza A (H1N1) 2009 virus infection. *Clin Infect Dis* **52:447-456.**
- 572 18. **Chan KH, To KK, Hung IF, Zhang AJ, Chan JF, Cheng VC, Tse H, Che XY,**
573 **Chen H, Yuen KY.** 2011. Differences in antibody responses of individuals with
574 natural infection and those vaccinated against pandemic H1N1 2009 influenza. *Clin*
575 *Vaccine Immunol* **18:867-873.**

- 576 19. **Vella S, Rocchi G, Resta S, Marcelli M, De Felici A.** 1980. Antibody reactive in
577 antibody-dependent cell-mediated cytotoxicity following influenza virus vaccination.
578 *J Med Virol* **6**:203-211.
- 579 20. **Zaritskaya L, Shurin MR, Sayers TJ, Malyguine AM.** 2010. New flow cytometric
580 assays for monitoring cell-mediated cytotoxicity. *Expert Rev Vaccines* **9**:601-616.
- 581 21. **Lau SK, Chan KH, Yip CC, Ng TK, Tsang OT, Woo PC, Yuen KY.** 2009.
582 Confirmation of the first Hong Kong case of human infection by novel swine origin
583 influenza A (H1N1) virus diagnosed using ultrarapid, real-time reverse transcriptase
584 PCR. *J Clin Microbiol* **47**:2344-2346.
- 585 22. **Chao G, Lau WL, Hackel BJ, Sazinsky SL, Lippow SM, Wittrup KD.** 2006.
586 Isolating and engineering human antibodies using yeast surface display. *Nat Protoc*
587 **1**:755-768.
- 588 23. **Gietz RD, Schiestl RH.** 2007. High-efficiency yeast transformation using the
589 LiAc/SS carrier DNA/PEG method. *Nat Protoc* **2**:31-34.
- 590 24. **Weng WK, Levy R.** 2003. Two immunoglobulin G fragment C receptor
591 polymorphisms independently predict response to rituximab in patients with follicular
592 lymphoma. *J Clin Oncol* **21**:3940-3947.
- 593 25. **Shields RL, Namenuk AK, Hong K, Meng YG, Rae J, Briggs J, Xie D, Lai J,
594 Stadlen A, Li B, Fox JA, Presta LG.** 2001. High resolution mapping of the binding
595 site on human IgG1 for Fc gamma RI, Fc gamma RII, Fc gamma RIII, and FcRn and
596 design of IgG1 variants with improved binding to the Fc gamma R. *J Biol Chem*
597 **276**:6591-6604.
- 598 26. **Schlaeth M, Berger S, Derer S, Klausz K, Lohse S, Dechant M, Lazar GA,
599 Schneider-Merck T, Peipp M, Valerius T.** 2010. Fc-engineered EGF-R antibodies
600 mediate improved antibody-dependent cellular cytotoxicity (ADCC) against KRAS-
601 mutated tumor cells. *Cancer Sci* **101**:1080-1088.
- 602 27. **Nimmerjahn F, Ravetch JV.** 2007. Antibodies, Fc receptors and cancer. *Curr Opin*
603 *Immunol* **19**:239-245.
- 604 28. **Zhang W, Gordon M, Schultheis AM, Yang DY, Nagashima F, Azuma M, Chang
605 HM, Borucka E, Lurje G, Sherrod AE, Iqbal S, Groshen S, Lenz HJ.** 2007.
606 FCGR2A and FCGR3A polymorphisms associated with clinical outcome of
607 epidermal growth factor receptor expressing metastatic colorectal cancer patients
608 treated with single-agent cetuximab. *J Clin Oncol* **25**:3712-3718.
- 609 29. **Ferrari G, Pollara J, Kozink D, Harms T, Drinker M, Freel S, Moody MA, Alam
610 SM, Tomaras GD, Ochsenauber C, Kappes JC, Shaw GM, Hoxie JA, Robinson
611 JE, Haynes BF.** 2011. An HIV-1 gp120 envelope human monoclonal antibody that
612 recognizes a C1 conformational epitope mediates potent antibody-dependent cellular
613 cytotoxicity (ADCC) activity and defines a common ADCC epitope in human HIV-1
614 serum. *J Virol* **85**:7029-7036.
- 615 30. **Bonsignori M, Pollara J, Moody MA, Alpert MD, Chen X, Hwang KK, Gilbert
616 PB, Huang Y, Gurley TC, Kozink DM, Marshall DJ, Whitesides JF, Tsao CY,
617 Kaewkungwal J, Nitayaphan S, Pitisuttithum P, Rerks-Ngarm S, Kim JH,
618 Michael NL, Tomaras GD, Montefiori DC, Lewis GK, Devico A, Evans DT,
619 Ferrari G, Liao HX, Haynes BF.** 2012. Antibody-Dependent Cellular Cytotoxicity-
620 Mediating Antibodies from an HIV-1 Vaccine Efficacy Trial Target Multiple
621 Epitopes and Preferentially Use the VH1 Gene Family. *J Virol* **86**:11521-11532.
- 622 31. **Hashimoto G, Wright PF, Karzon DT.** 1983. Antibody-dependent cell-mediated
623 cytotoxicity against influenza virus-infected cells. *J Infect Dis* **148**:785-794.
- 624 32. **Neiryneck S, Deroo T, Saelens X, Vanlandschoot P, Jou WM, Fiers W.** 1999. A
625 universal influenza A vaccine based on the extracellular domain of the M2 protein.
626 *Nat Med* **5**:1157-1163.

- 627 33. **El Bakkouri K, Descamps F, De Filette M, Smet A, Festjens E, Birkett A, Van**
628 **Rooijen N, Verbeek S, Fiers W, Saelens X.** 2011. Universal vaccine based on
629 ectodomain of matrix protein 2 of influenza A: Fc receptors and alveolar macrophages
630 mediate protection. *J Immunol* **186**:1022-1031.
- 631 34. **Brunner KT, Mauel J, Cerottini JC, Chapuis B.** 1968. Quantitative assay of the
632 lytic action of immune lymphoid cells on 51-Cr-labelled allogeneic target cells in
633 vitro; inhibition by isoantibody and by drugs. *Immunology* **14**:181-196.
- 634 35. **Umana P, Jean-Mairet J, Moudry R, Amstutz H, Bailey JE.** 1999. Engineered
635 glycoforms of an antineuroblastoma IgG1 with optimized antibody-dependent cellular
636 cytotoxic activity. *Nat Biotechnol* **17**:176-180.
- 637 36. **Velders MP, van Rhijn CM, Oskam E, Fleuren GJ, Warnaar SO, Litvinov SV.**
638 1998. The impact of antigen density and antibody affinity on antibody-dependent
639 cellular cytotoxicity: relevance for immunotherapy of carcinomas. *Br J Cancer*
640 **78**:478-483.
641
642

FIG 1

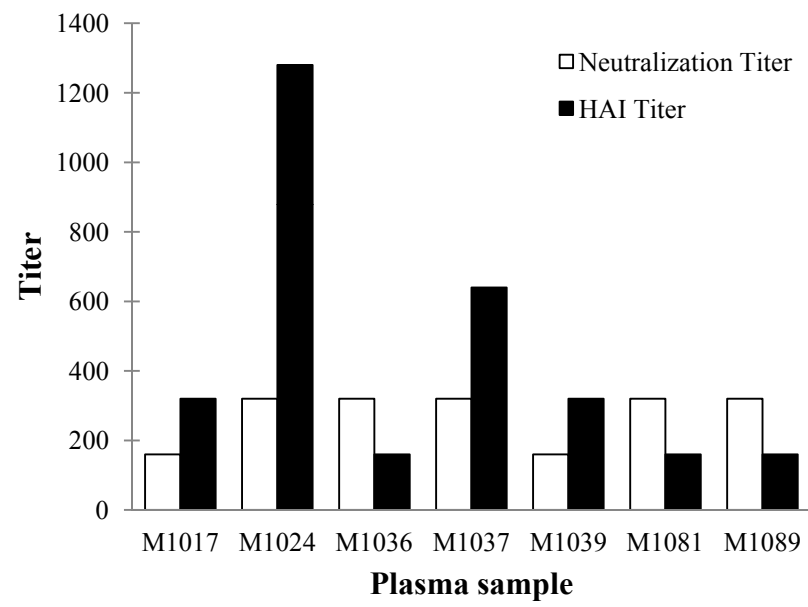


FIG 2

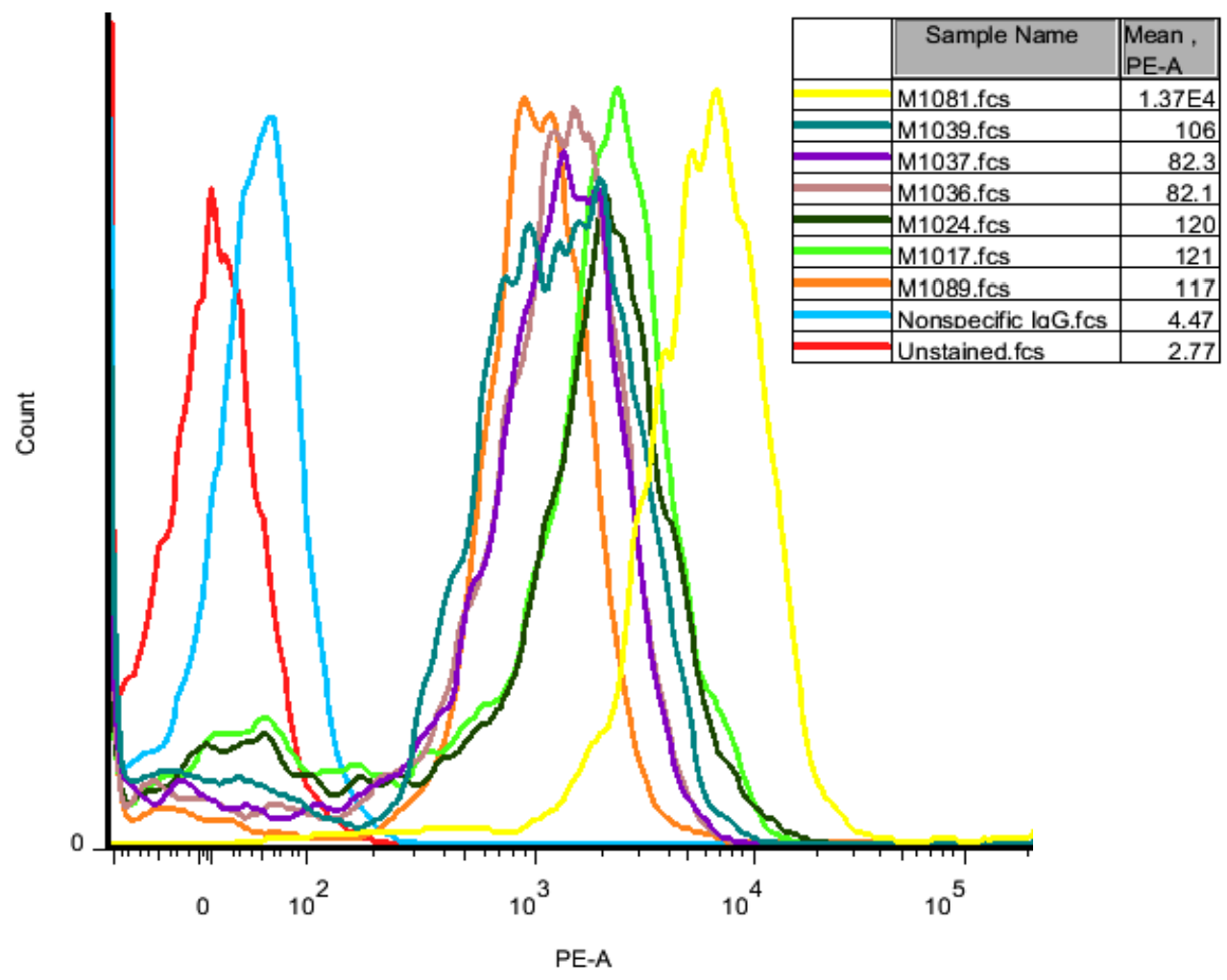


FIG 3

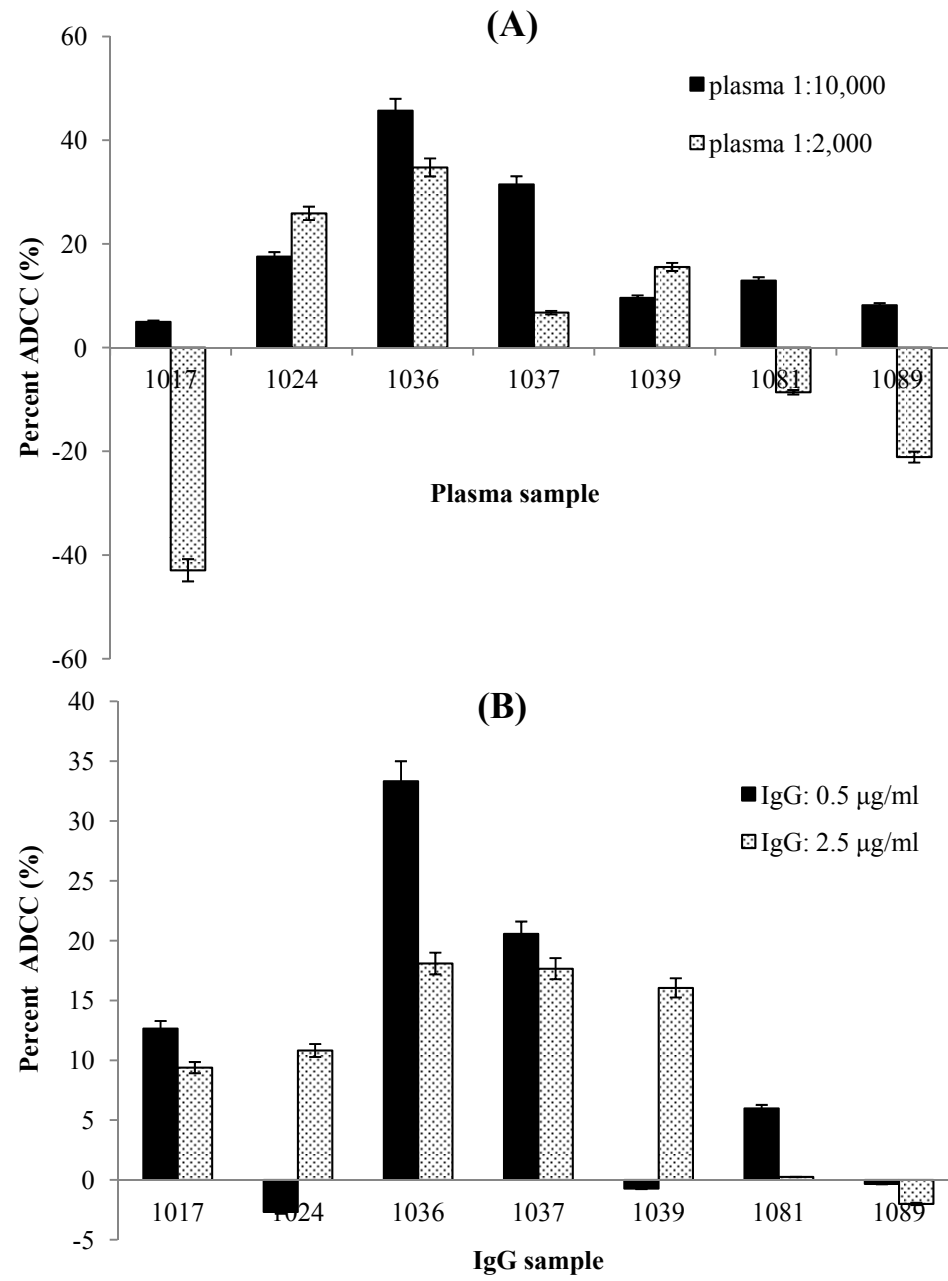


FIG 4

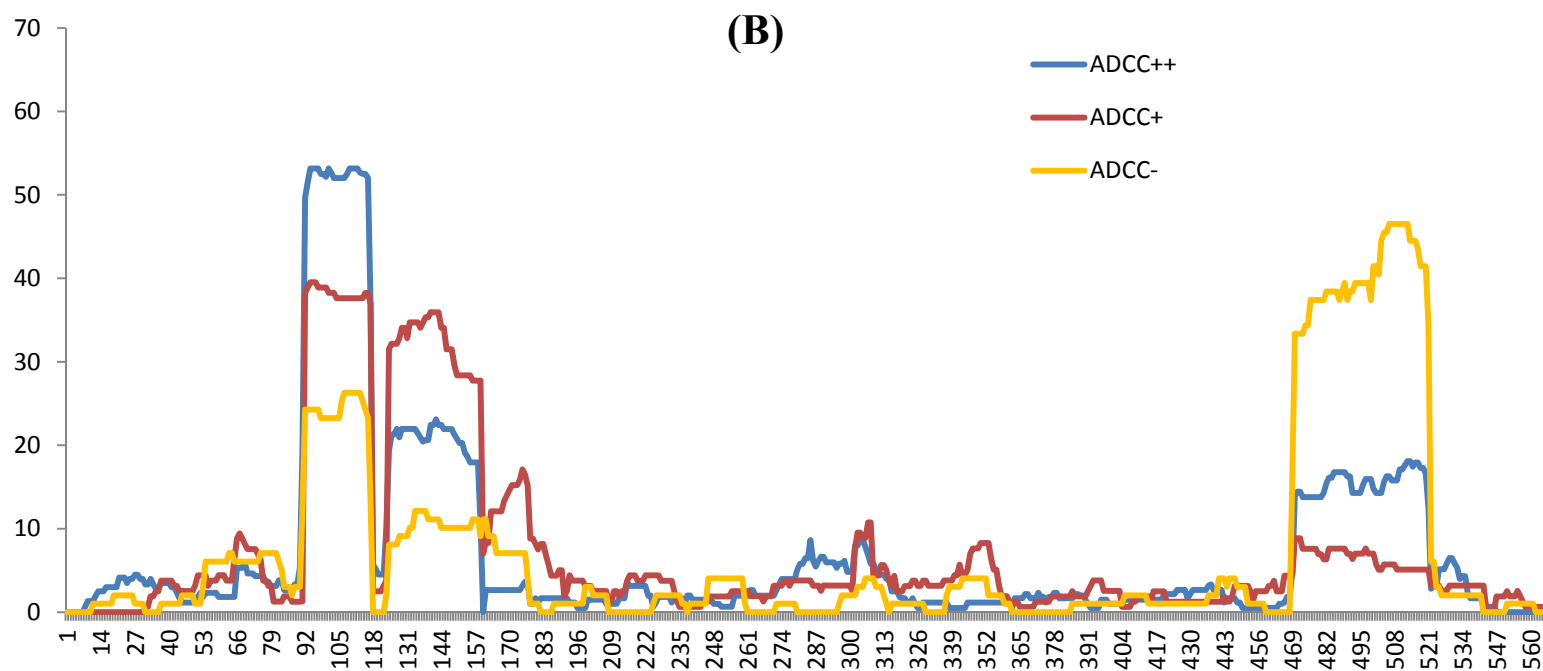
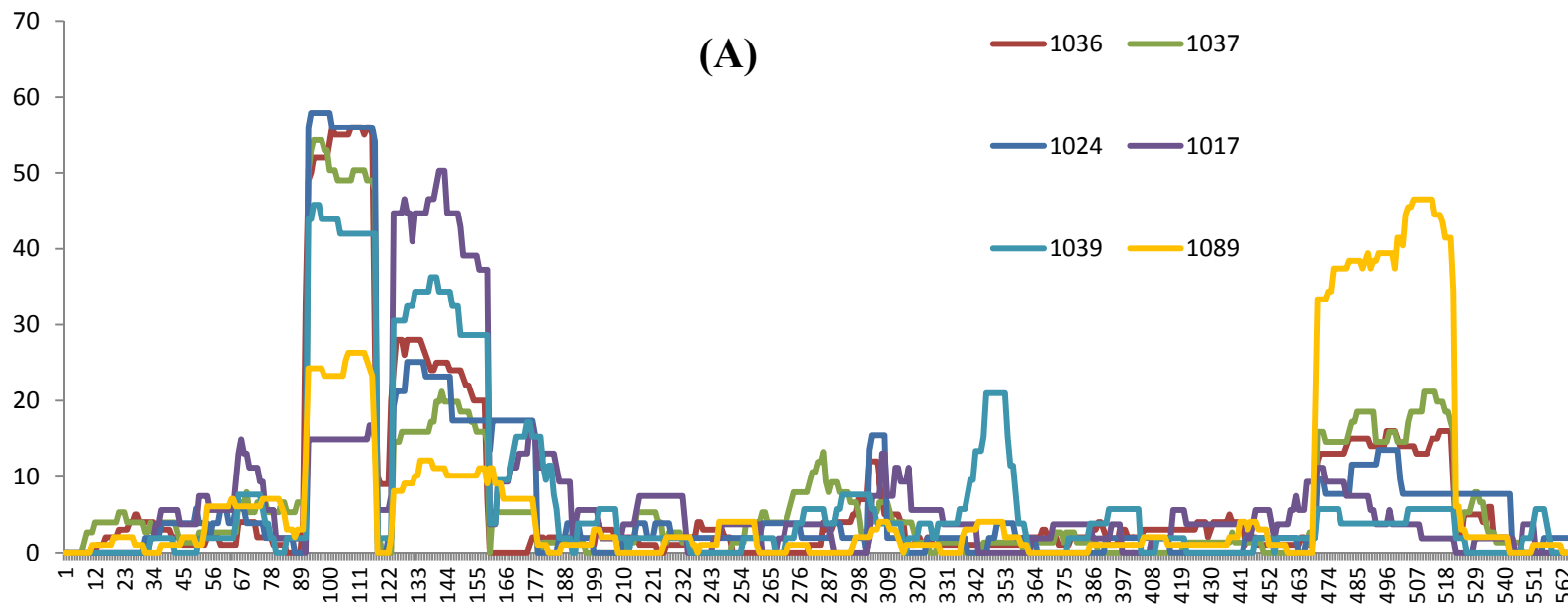


FIG 5

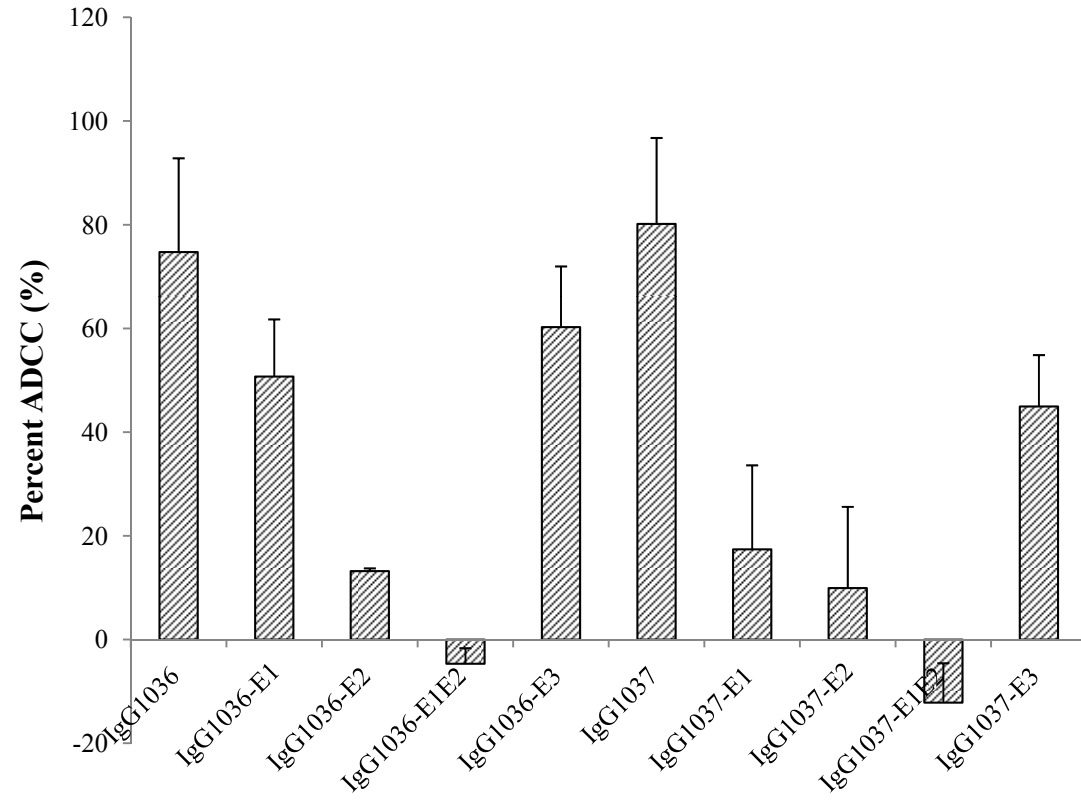


TABLE 1 Average AA frequency of three immunodominant epitopes on H1N1 HA.

HA Epitopes	AA position	AA Sequence	Average AA Frequency		
			ADCC++ (M1036 and M1037)	ADCC+ (M1024, M1017 and M1039)	ADCC- (M1089)
HA-E1	92-117	SWSYIVETSSSDNGTCYPGDFI DYEE	51.86±3.16	38.21±0.72	24.11±2.55
HA-E2	124-159	SVSSFERFEIFPKISSWPNHESN KGVTAACPHAGAK	20.66±2.23	32.14±2.93	10.25±1.19
HA-E3	470-521	LKNNAKEIGNGCFEFYHKCDN TCMESVKNGTYPKYSEEA KLNREEIDGVK	15.57±1.45	6.54±1.17	40.17±4.09

